Interaction between $Pt(acac)_2$ and alumina surfaces studied by XAS

M. Womes [a,*], J. Lynch [a], D. Bazin [b], F. Le Peltier [a], S. Morin [a], and B. Didillon [a]

[a] Institut Français du Pétrole, 1&4 av. de Bois Préau, BP 311, 92506 Rueil-Malmaison, France
[b] Laboratoire pour l'Utilisation du Rayonnement Electromagnétique LURE, Université Paris Sud, Bâtiment 209, 94105 Orsay, France

Received 7 May 2002; accepted 17 September 2002

The anchoring and decomposition mechanisms of platinum(II) bis-acetylacetonate on alumina surfaces are studied by X-ray absorption spectroscopy at the platinum L_{III} edge. A distinction is made between highly reactive surfaces which are partially dehydroxylated and exhibit coordinatively unsaturated surface sites, and deactivated surfaces which are covered by a monolayer of OH groups. The samples are studied after three stages of a wet impregnation synthesis: after drying at room temperature, drying at 120 °C and calcination at 350 °C. The XANES signal and the filtered EXAFS signals of the first and second coordination shells around platinum were analyzed. Two different mechanisms are discussed for the two types of supports.

KEY WORDS: XANES; EXAFS; synthesis; platinum-based catalysts.

1. Introduction

Supported metals are extensively used in industry to catalyze various chemical reactions. Their catalytic properties are determined by several parameters, like particle size, dispersion, etc. It is obvious that the reproducible preparation of well-defined catalysts with predefined properties needs a detailed knowledge of the mechanisms controlling the reaction between the metal precursor and the surface of the support. The currently widely used Pt/Al_2O_3 catalysts are often prepared by wet impregnation techniques using as metal precursor a salt, like H_2PtCl_6, or an organometallic complex, like platinum(II) bis-acetylacetonate ($Pt(acac)_2$). The wet impregnation technique comprises three steps: (i) the impregnation step, where the support is brought into contact with a solution containing the precursor; (ii) a drying step where, after extraction from the solution, the solvent remaining in the pores of the support is evaporated at temperatures around 100 °C; and (iii) a calcination step, where the initial ligands are removed from the metal while it is definitively fixed to the support by chemical bonds with surface oxygen atoms. While the mechanisms governing these three steps have been investigated in detail for the precursor H_2PtCl_6 [1,2], little is known about the way $Pt(acac)_2$ adsorbs and decomposes on alumina surfaces. Berdala *et al.* [3] studied Pt/Al_2O_3 catalysts prepared from $Pt(acac)_2$ after drying, calcination and reduction steps at various temperatures. These authors proposed a two-step decomposition mechanism with the loss of one acac ligand at the drying stage and platinum bonded to two or three surface oxygen atoms, and the loss of the second acac ligand during the calcination step. Similar mechanisms were proposed for $Pd(acac)_2$ [4] and $Ni(acac)_2$ [5] on alumina and $Cu(acac)_2$, $Pd(acac)_2$ and $Pt(acac)_2$ on silica [6–8]. An alternative model was proposed by van Veen *et al.* [9]. According to these authors an immediate complete decomposition of $Pd(acac)_2$ and $Pt(acac)_2$ occurs on coordinatively unsaturated surface (c.u.s.) aluminum ions following the equation

$$Pd(acac)_2 + Al_s^{3+} \longrightarrow [Al(acac)_x]_s^{(3-x)^+} + Pd_s^{2+}$$

where s denotes a surface site the exact environment of which has not been further specified. The authors observed an increasing amount of metal adsorbed with increasing degree of dehydroxylation of the surface. At high metal loadings physisorption of $Pt(acac)_2$ was observed on some but not all of the supports used in their study. Low metal loadings led to inhomogeneous, eggshell-like metal distributions across the alumina pellets.

The work on H_2PtCl_6 [1,2] showed that the interaction mechanism depends critically on the nature of the sites present at the surface of the support, a point that remained beyond the scope of several of the studies cited above. Alumina surfaces exposed to water or moist atmospheres are terminated by a monolayer of hydroxyl groups. Dehydroxylation by heat treatments leaves c.u.s. aluminum ions in the outermost surface layer which are electron deficient and behave therefore as a Lewis acid site [10–12].

The purpose of the present study is to further elucidate the reaction mechanism between $Pt(acac)_2$ and alumina surfaces. A distinction is made between the aforementioned two types of alumina surfaces. We chose X-ray absorption spectroscopy (XAS) at the Pt L_{III} edge to

* To whom correspondence should be addressed. Present address: Université Montpellier II, LAMMI, CC015, Place E. Bataillon, F-34095 Montpellier Cedex 5, France.

1011-372X/03/0100-0025/0

follow the progressive decomposition of the complex and the anchoring of the metal on the surface. Analysis of the X-ray absorption near-edge structure (XANES) provides information on the oxidation state of the probing atom by means of the intensity of the white line [13,14]. Evaluation of the extended X-ray absorption fine structure (EXAFS) gives insight into the local environment of the probed element on an atomic scale. XAS is therefore well suited to study isolated molecules adsorbed on surfaces [15–18]. Our study comprises an analysis of the white line intensity and the EXAFS signals of both the first and second coordination shell around platinum atoms of samples dried at 25 and 120 °C and calcined at 350 °C, corresponding to the three steps of the impregnation technique mentioned above.

2. Experimental

2.1. Preparation of high-dispersion catalysts

The alumina support used consisted of pellets of γ_c-alumina with a diameter of 2 mm and a pore volume of 0.6 cm^3/g. Two methods of surface pre-treatment prior to impregnation were used:

(i) Calcination of the support for 2 h at 350 °C in a dry air stream, followed by cooling to room temperature overnight in the same air stream. In the following, a support treated in this way will be referred to as a reactive support.
(ii) Hydroxylation by incipient wetness impregnation with an amount of water corresponding to the pore volume of the pellets. The support was then dried at 120 °C overnight. No calcination prior to the impregnation was carried out. These supports will be referred to as deactivated supports.

Immediately after the pre-treatment, the supports were impregnated during 24 h at room temperature with $Pt(acac)_2$ (Johnson Matthey, >98.8%) diluted in toluene, with a solvent to support ratio of 5 ml/g. The catalysts were then filtered and washed in toluene. Two series of samples were prepared, one on a reactive and one on a deactivated support. The initial $Pt(acac)_2$ concentration was 1 mM. Three samples were taken from each preparation. The first was dried after impregnation in ambient atmosphere at 25 °C, the second also in ambient atmosphere at 120 °C, the third was calcined at 350 °C in a dry air stream. In the following these samples are referred to as "D" and "R" for the deactivated and reactive support, respectively, followed by the temperature at which they were dried.

2.2. XAS

XAS spectra were recorded in the Laboratoire pour l'Utilisation du Rayonnement Electromagnétique, Orsay, at the EXAFS4 beam line using synchrotron radiation from the DCI storage ring running at 1.85 GeV with an average current of 250 mA. The XAS data were recorded at the Pt L_{III} absorption edge at about 11560 eV in transmission geometry, using a Si(111) double-crystal monochromator. The energy step width was 0.5 eV in the XANES region (11540–11585 eV) and 3 eV in the EXAFS region. The time necessary to measure a complete X-ray absorption spectrum (11450–12300 eV) was about 25 min.

For analysis of the XANES region, the Pt L_{III} edge spectra were first corrected for a linear baseline and then for atomic absorption by fitting a polynomial function to the spectral region above the absorption edge. The spectra were normalized with respect to the point at 12300 eV, where EXAFS oscillations are already completely attenuated. EXAFS spectra were analyzed using a standard data analysis procedure [19] (SIMPLEX software package [20]). The EXAFS spectrum was first transformed from k space (k^3, Hanning windows 3.28, 4.2, 10.4, 12 $Å^{-1}$) to R space to obtain the radial distribution function $f(R)$. The EXAFS spectrum for one or several coordination shells was isolated by inverse Fourier transform of $f(R)$ over the appropriate region and fitted using the single-scattering EXAFS equation. Phase and amplitude functions were derived from the spectrum of $Pt(acac)_2$ using as parameters $N = 4$ for the number of first neighbors and $d = 1.99$ Å for the Pt–O distance [21].

The experimental error in the determination of the absorption coefficient at the white line maximum, essentially induced by the normalization procedure, is estimated as ±0.05 units, the error in N, the number of neighbors in the first coordination shell, as ±0.5 and the error in R as ±0.02 Å.

3. Results

3.1. XANES

The values of the absorption coefficient μ at the white line maximum with respect to the normalization point at 12300 eV are given in table 1. The line widths, measured at half height from the maximum, show no significant differences between the reference compounds and all samples, so that the analysis of the line shape can be limited to a comparison of the peak heights. The

Table 1
X-ray absorption coefficient at the Pt L_{III} edge white line maximum with respect to the normalization point at 12300 eV

$Pt(acac)_2$	1.28		
D25	1.43	R25	1.47
D120	1.43	R120	1.52
D350	1.70	R350	1.75
PtO_2	1.70		

formal oxidation state of platinum in Pt(acac)$_2$ is +2, corresponding to a formal electron configuration of $5d^8$, whereas in PtO_2 platinum is usually described as Pt(IV) with an electron configuration of $5d^6$. The white line intensities of the two compounds reflect well the higher number of unoccupied d states in Pt(IV) as compared to Pt(II).

The evolution of the white line intensity in the series of samples R25 to R350 indicates a progressive oxidation of the metal with increasing temperature of the heat treatment. The line intensities of D25 and D120 are identical and somewhat lower than that of R25 but still higher than that of bulk Pt(acac)$_2$, which gave the lowest intensity of all samples studied. Comparison of samples D350 and R350 with PtO_2 shows that, independent of the surface pre-treatment, after calcination at 350 °C all platinum is in the +4 oxidation state.

3.2. EXAFS first coordination shell

As outlined in the introduction, the number of neighboring atoms around the absorber is derived from the intensity of the EXAFS oscillations above the absorption edge. Figure 1 shows as an example the extracted EXAFS signal of sample D120. Spectra of similar quality (signal-to-noise ratio S/N) were obtained for all samples with the exception of R120, where the S/N ratio was somewhat lower.

When analyzing an EXAFS signal, it must be kept in mind that the oscillation intensities, and thus also the magnitude of $f(R)$, are reduced by atomic disorder and atomic vibrations. This is usually corrected for by comparison with a crystallographically well-defined reference compound of similar structure. In the present case, the samples consist of isolated molecules while the reference compound is bulk Pt(acac)$_2$. It is obvious that atomic vibrations in adsorbed molecules are different from

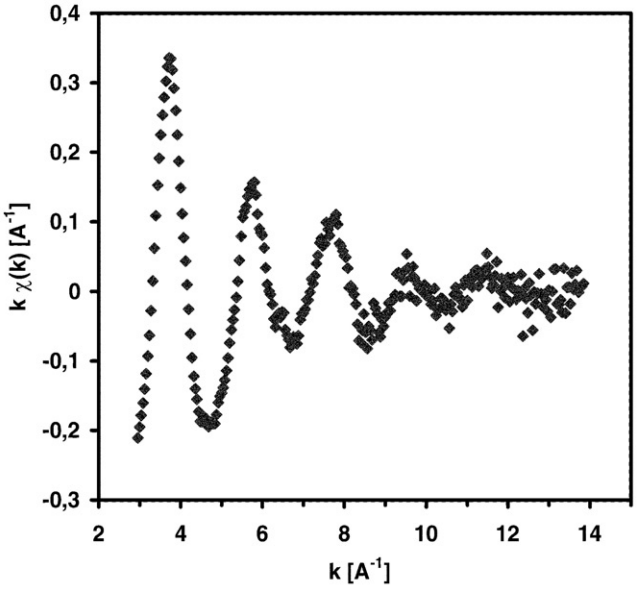

Figure 1. EXAFS signal of sample D120.

those in bulk material and must be corrected for if true coordination numbers are to be obtained. For systems with the same atomic neighbors at the same distance:

$$\chi(k) \propto N\, e^{-2k^2\sigma^2}$$

where N is the number of neighbors and σ is a term representing the disorder. The function χ_{ref} for platinum bisacetylacetonate corresponds to four neighbors so that

$$\ln\left[\frac{\chi(k)}{\chi_{ref}(k)}\right] = \ln\left[\frac{N}{4}\right] + 2k^2(\sigma_{ref}^2 - \sigma^2)$$

and a plot of $\ln(\chi/\chi_{ref})$ vs. k^2 will be a straight line with an intercept at $k=0$ of $\ln(N/4)$ [22]. The value of N obtained by this method is independent of disorder. Examples of plots of $\ln(\chi/\chi_{ref})$ vs. k^2 are shown in figure 2 and derived values for coordination number

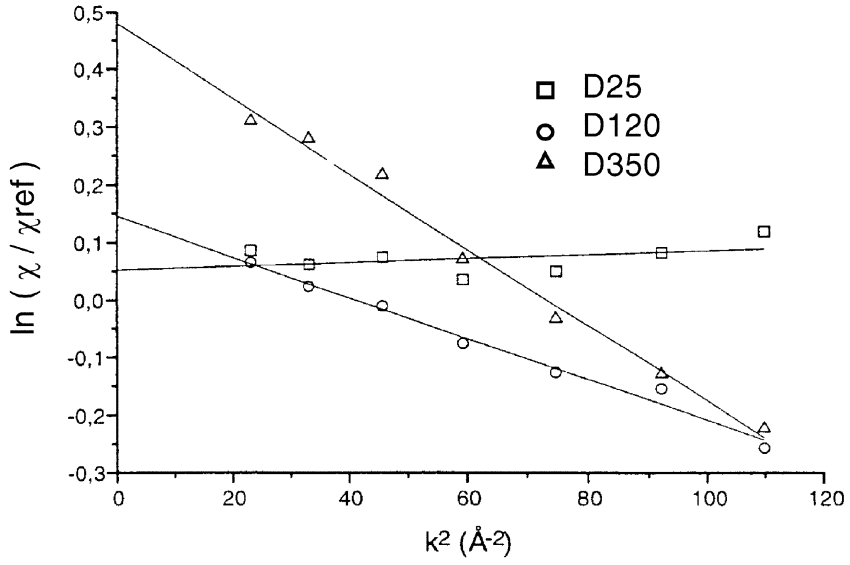

Figure 2. Determination of structural parameters from EXAFS data of Pt(acac)$_2$ impregnated on deactivated (D) supports dried at 25, 120 and 350 °C.

Table 2
Coordination numbers N and disorder parameter $\Delta\sigma^2$ derived from the filtered first coordination shell EXAFS signal as shown in figure 3. R values were determined from a fit to the filtered Fourier-transformed signals of the first coordination shell

Sample	N (oxygen)	$\Delta\sigma^2$ (10^{-3} Å^2)	R (Å)
R25	4.6	2	2.00
R350	6.9	6	2.03
D25	4.2	−0.3	2.00
D120	4.3	3	2.00
D350	6.5	6	2.01

and relative disorder are presented in table 2. The spectrum for R120 was not evaluated due to poor signal-to-noise ratio.

Sample D25 shows N and σ values close to those of $Pt(acac)_2$. For D120 we find a similar value for N and a higher value of σ. Sample R25 also shows an increased disorder with respect to $Pt(acac)_2$, with a value of σ very similar to that of D120. For samples D350 and R350 we find values of N close to 6, the coordination number of platinum in PtO_2. Comparison of the radial distribution functions shows that the Pt–O distances in $Pt(acac)_2$, PtO_2 and the samples differ by no more than 0.04 Å, all lying in the range 1.99–2.03 Å. Differences in coordination number and first neighbor distances are obviously rather weak, making it difficult to distinguish between oxygen atoms of the acac group and oxygen atoms of the alumina surface. A deeper insight into the reaction mechanism can, in principle, be expected from an evaluation of the second coordination shell, where it should be possible to distinguish between carbon atoms of the acac group and aluminum atoms of the support.

3.3. EXAFS second coordination shell

The classical EXAFS theory is based on the assumption that the EXAFS signal beyond approximately 50 eV above the absorption edge is exclusively due to single scattering and free of any contributions from multiple scattering. A first step in the evaluation of the EXAFS signal of outer shells must be a verification of this hypothesis for the case under study. We used the FEFF7 code [23] to calculate all possible single and multiple scattering paths for $Pt(acac)_2$ up to path lengths of 5 Å using the crystallographic data of Onuma *et al.* [21]. The individual single-scattering contributions of the C and O atoms to $f(R)$ reproduce well the corresponding peaks in the experimental curve (figure 3), but do not reproduce the part between 3 and 4.5 Å, which the calculation shows to be essentially due to numerous multiple scattering paths. Some of these contribute as much intensity to the EXAFS signal as do the single-scattering paths. A conventional EXAFS code must therefore fail to simulate correctly the $Pt(acac)_2$ EXAFS spectrum of the second coordination shell and the evaluation of the data must be limited to a comparison with bulk $Pt(acac)_2$ by visual inspection. This will be done in the following by comparison of the filtered EXAFS signals of the range 2.2–4.5 Å (figure 4).

The following remarks can be made. An oscillation beat at 5 Å^{-1} in the filtered EXAFS signal of bulk $Pt(acac)_2$ can be explained by interference of the

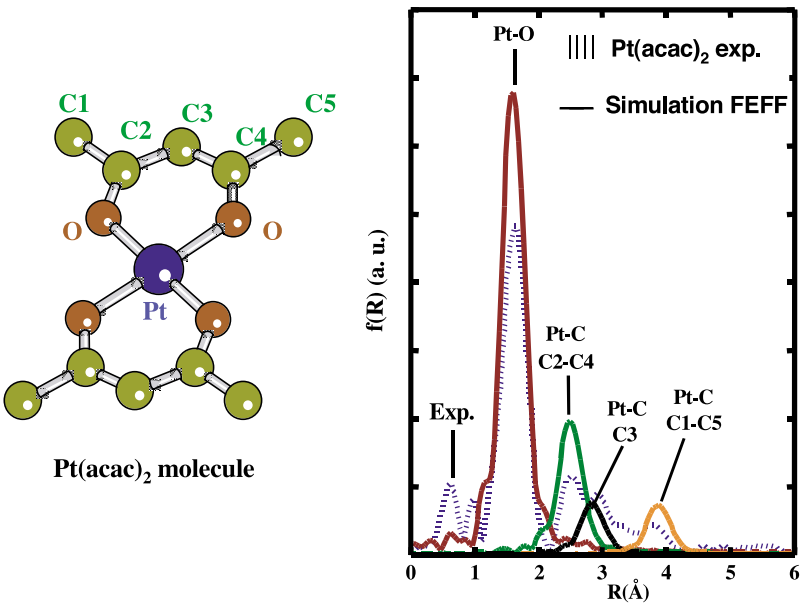

Figure 3. Numbering of atoms in the acac cycle (left) and FEFF simulation of contributions to $f(R)$ from single scattering compared to the experimental $f(R)$ curve of $Pt(acac)_2$ (right).

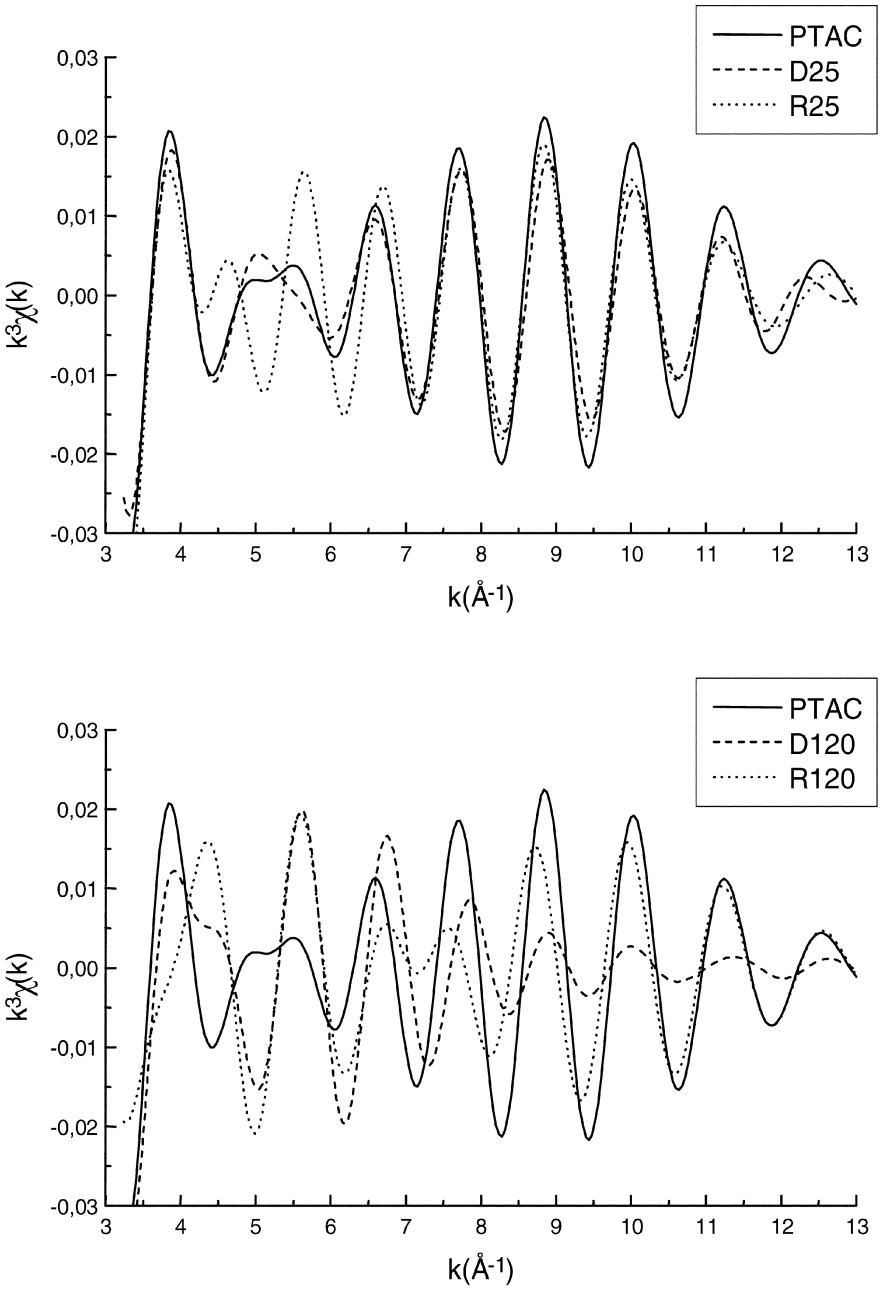

Figure 4. Filtered EXAFS signal (2.2–4.5 Å) of bulk $Pt(acac)_2$ and the catalyst samples.

backscattered waves from the carbon atoms at three different distances. The filtered EXAFS signal of D25 agrees well in shape with that of bulk $Pt(acac)_2$, indicating that the atomic arrangement of the complex is entirely conserved. Samples R25, R120 and D120 are clearly different from $Pt(acac)_2$ indicating a modification of the atomic arrangement in the second coordination shell. The main difference between samples R25 and D120 on one side and $Pt(acac)_2$ on the other is a shift of the oscillation beat from 5 to 4.5 $Å^{-1}$. This oscillation beat is more pronounced in D120 and the oscillations fade out more rapidly than in R25. R120 is different from all other samples showing an oscillation beat at 7 $Å^{-1}$.

It is worth noting that no Pt–Pt second neighbors are detected in the $f(R)$ of any of the samples, showing that the platinum remains in a dispersed state.

4. Discussion

The first- and second-shell EXAFS results of D25 agree well with those of $Pt(acac)_2$. The complex remains intact and is anchored by physisorption, as already observed for hydroxylated silica surfaces [6]. Kenvin *et al.* proposed for this latter case an interaction by hydrogen bonding either between the oxygen atoms of the acac ligand or by the π-electron system of the

whole chelate ring and the OH groups of the surface [6,7]. Such an interaction is likely to also affect the Pt–O bond properties by withdrawing electron density from the metal towards the ligands. This would explain the higher density of unoccupied 5d states in the supported complexes as compared to bulk $Pt(acac)_2$, as is reflected by the increased intensity of the white line of D25 with respect to the reference sample.

Heating to 120 °C leads to a decomposition of at least some of the complexes with modification of the second Pt coordination shell. The higher disorder in the first coordination shell at constant mean coordination and electron numbers can be explained by platinum bonds to oxygen atoms of the support replacing those of one or both acac ligands.

The second coordination shell of R25 is also clearly different from that of $Pt(acac)_2$. The interaction of electron-deficient surface sites with the chelate ring is sufficiently strong to lead to an immediate decomposition of the complex already at room temperature. Once all c.u.s. sites are saturated in this way, further complexes from the solution are physisorbed as described for D25. R25 also differs from D120. In addition to different second coordination shells, we see slight increases in the mean Pt coordination number and oxidation state with respect to D120 (or D25). For sample R120 the change in the mean Pt electron configuration with respect to D120/D25 is still more pronounced. Heating to 120 °C increases the fraction of decomposed complexes.

Calcination at 350 °C causes a definitive decomposition of the $Pt(acac)_2$ complex leading to a local environment close to that of PtO_2, independent of the way the surface was pre-treated. Deviations from the ideal oxygen coordination value of six may be explained by the fact that the phase and amplitude functions for scattering derived from $Pt(acac)_2$ as reference compound differ from those in PtO_2.

These results demonstrate that the decomposition of the $Pt(acac)_2$ complex on alumina surfaces follows two different mechanisms:

(i) an immediate, chemically induced decomposition at room temperature on c.u.s. sites of partially dehydroxylated surfaces; and
(ii) a thermally induced decomposition below 120 °C of complexes loosely bound to surface OH groups.

The Pt–O distances for platinum bound in the complex and bound to surface oxygen atoms are too similar to be detected separately; EXAFS provides here no information on the fraction of decomposed versus physisorbed intact complexes. It is therefore difficult to confirm from the present data the model of an immediate complete decomposition on c.u.s. sites, as proposed by van Veen *et al*. [9] or a two-step mechanism as proposed by several other authors [3–8]. The results indicate, however, that the decomposition mechanisms (i) and (ii) mentioned above involve surface sites that differ by more than the presence or absence of one OH group. Decomposition on a reactive support is accompanied by an increase of coordination number and oxidation state, leading to hexa-coordinated Pt(IV). Decomposition on a deactivated support at temperatures below 120 °C rather conserves tetra-coordinated Pt(II). Calcination of the support at 350 °C might create several neighboring c.u.s. sites, allowing platinum to form bonds with a larger number of surface oxygens than on a deactivated support where drying at 120 °C does not create such sites.

The consequences of the above observations for catalyst synthesis by wet impregnation techniques are obvious. An immediate decomposition of the complex upon the first contact with the surface of the support, especially when the lost acac ligand – or both lost ligands – react themselves with the alumina surface as seen by van Veen *et al*. [9], must shift the equilibrium between complexes in solution and on the surface completely towards the surface. Therefore, sample preparations with low metal loads on highly reactive surfaces lead to inhomogeneous, i.e. eggshell-like, metal distributions across the porous support particles, as observed by van Veen *et al*. [9]. The metal is deposited on the outermost shell of the particles where the solution first comes in contact with the support. On the other hand, the rather weak interaction with a deactivated surface, leaving the complex intact, should allow for an equilibrium that is not completely shifted toward the surface. In this way, homogeneous metal distributions even for low metal loads are obtained.

5. Conclusion

Anchoring and decomposition of platinum(II) bis-acetylacetonate on alumina surfaces has been studied by X-ray absorption spectroscopy at the platinum L_{III} edge. The interaction between $Pt(acac)_2$ and deactivated (i.e. hydroxylated) alumina surfaces is weak and causes no destruction of the complex upon contact with the support. Anchoring on the surface is made by simple physisorption. Heating to 120 °C leads to a decomposition of a fraction of the complexes. The interaction with reactive (i.e. coordinatively unsaturated) surface sites is strong and leads to an immediate decomposition of the complex at room temperature upon the first contact. The results indicate that decomposition on reactive and deactivated surfaces anchors the metal on surface sites of different nature, leading to different coordination spheres. Calcination at 350 °C in dry air leads to a complete decomposition of all complexes, to an oxidation of all platinum to Pt(IV) and to PtO_2-like particles. No Pt–Pt second neighbors are detected in the radial distribution function of any of the samples, showing that the platinum remains in a dispersed state.

The study further demonstrates the usefulness of EXAFS in studying reaction mechanisms between single molecules and surfaces. A careful analysis of the EXAFS signal in terms of single and multiple scattering is, however, to be carried out prior to investigations beyond the first coordination shell to make sure that the basic assumption of EXAFS theory of negligible contributions from multiple scattering is valid for the second and outer coordination shells.

References

[1] J. Berdala, E. Freund and J.P. Lynch, J. Physique 47 (1986) C8-269.
[2] B. Shelimov, J.F. Lambert, M. Che and B. Didillon, J. Catal. 185 (1999) 462.
[3] J. Berdala, E. Freund and J.P. Lynch, J. Physique 47 (1986) C8-265.
[4] E. Lesage-Rosenberg, G. Vlaic, H. Dexpert, P. Lagarde and E. Freund, Appl. Catal. 22 (1986) 211.
[5] M. Lindblad, L.P. Lindfors and T. Suntola, Catal. Lett. 27 (1994) 323.
[6] J.C. Kenvin, M.G. White and M.B. Mitchell, Langmuir 7 (1991) 1198.
[7] J.C. Kenvin and M.G. White, J. Catal. 130 (1991) 447.
[8] M.B. Mitchell, V.R. Chakravarthy and M.G. White, Langmuir 10 (1994) 4523.
[9] J.A.R. van Veen, G. Jonkers and W.H. Hesselink, J. Chem. Soc. Faraday Trans. I 85 (1989) 389.
[10] J.B. Peri, J. Phys. Chem. 69 (1965) 220.
[11] H. Knözinger and P. Ratnasamy, Catal. Rev. Sci. Eng. 17 (1978) 31.
[12] H. Knözinger, Adv. Catal. 25 (1976) 184.
[13] F.W. Lytle, J. Catal. 43 (1976) 376.
[14] F.W. Lytle, P.S.P. Wei, R.B. Greegor, G.H. Via and J.H. Sinfelt, J. Chem. Phys. 70 (1979) 4849.
[15] D.C. Koningsberger and R. Prins (eds.), *X-ray Absorption*: *Principles*, *Applications*, *Techniques of Exafs*, *Sexafs and Xanes* (Wiley, 1988).
[16] Y. Iwasawa (ed.), *Xas for Catalysts and Surfaces* (World Scientific, Singapore, 1995).
[17] G. Sankar and J. M. Thomas, Topics Catal. 8 (1999) 1.
[18] D. Bazin and L. Guczi, Recent Res. Devel. Phys. Chem. 3 (1999) 387.
[19] D. Bazin, H. Dexpert, P. Lagarde and J. Bournonville, J. Catal. 123 (1988) 86.
[20] A. Michalowicz, J. Phys. IV C2-7 (1997) 235.
[21] S. Onuma, K. Horioka, H. Inoue and S. Shibata, Bull. Chem. Soc. Jpn. 53 (1980) 2679.
[22] S.M. Hunter, in: *EXAFS Spectroscopy*, eds. B.K. Teo and D.C. Joy (Plenum Press, New York, 1981), p. 163.
[23] J.J. Rehr, S.I. Zabinsky and R.C. Albers, Phys. Rev. Lett. 69 (1992) 3397.